Supporting information for:

Measurement report: Radiocarbon reveals contrasting size distributions of black carbon from fossil fuels and biomass burning in Guangzhou, China

Nannan Wei[1,2], Buqing Xu[2*], Sanyuan Zhu[2], Lingxiao Lu[2, 3], Jing Li[2], Fan Jiang[4], Junwen Liu[5], Zhineng Cheng[2], Shizhen Zhao[2], Kechang Li[2], Jun Li[2], Gan Zhang[2]

1 School of Nuclear Science and Technology, University of South China, Hengyang, Hunan, 421001, China

2 State Key Laboratory of Advanced Environmental Technology, Guangzhou Institute of Geochemistry, Chinese Academy of Sciences, Guangzhou, 510640, China

3 University of Chinese Academy of Sciences, Beijing, 100049, China

4 Key Laboratory of Ecological Environment Emergency and Sudden Risk Control, South China Institute of Environmental Sciences, Ministry of Ecology and Environment, Guangzhou 510655, PR China

5 Institute for Environmental and Climate Research, College of Environment and Climate, Jinan University, Guangzhou, 511443, China

This PDF file includes:

1. Supplementary Text (Text S1)

2. Supplementary Table (Table S1)

3. Supplementary Figure (Figure S1–S8)

Text S1. Calculation of secondary organic carbon and primary organic carbon

To further quantify the contribution of secondary production, secondary organic carbon (SOC) and primary organic carbon (POC) concentrations were estimated using the EC-tracer method:

$$POC = EC \times (OC/BC)_{min}$$

$$SOC = OC - POC$$

Here, BC denotes the EC fraction measured using the EUSAAR_2 thermal–optical protocol. $(OC/BC)_{min}$ represents the primary emission OC/BC ratio and was determined as 2.6 in this study based on the lowest observed OC/BC value.

Table S1. $\Delta^{14}C$ and $\delta^{13}C$ endmembers for the three source categories used in the Bayesian MCMC model. Values are presented as mean ± standard deviations.

	Biomass (C3 plants)	**Petroleum**	**Coal**
$\Delta^{14}C$ (‰)	38.1 ± 60.0	–1000	–1000
$\delta^{13}C$ (‰)	−28.8 ± 1.3	−25.3 ± 2.3	−23.8 ± 3.6

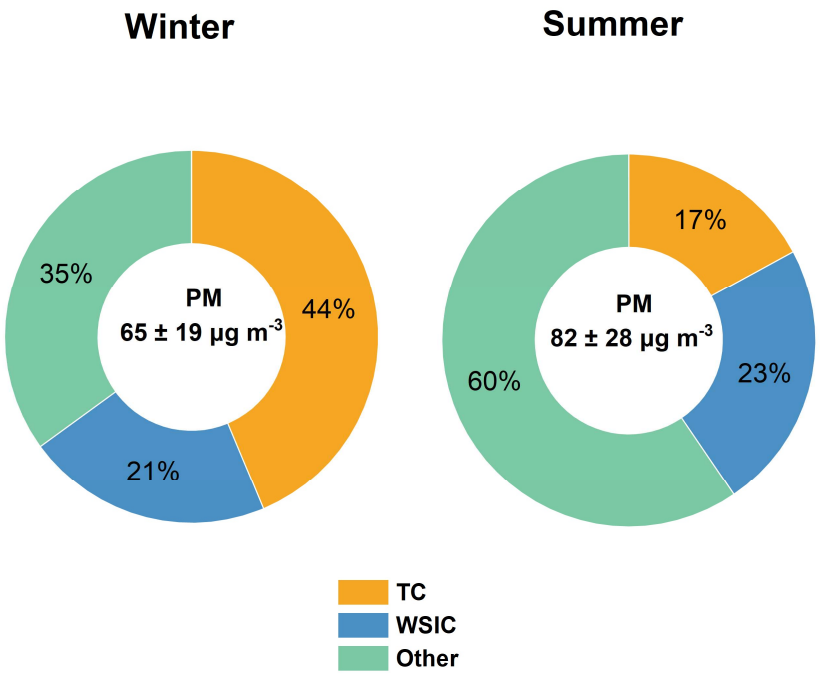


Figure S1. Mean relative contributions of total carbonaceous aerosol (TC), water-soluble inorganic ions (WSIC), and other components to total particulate matter (PM) during winter and summer.

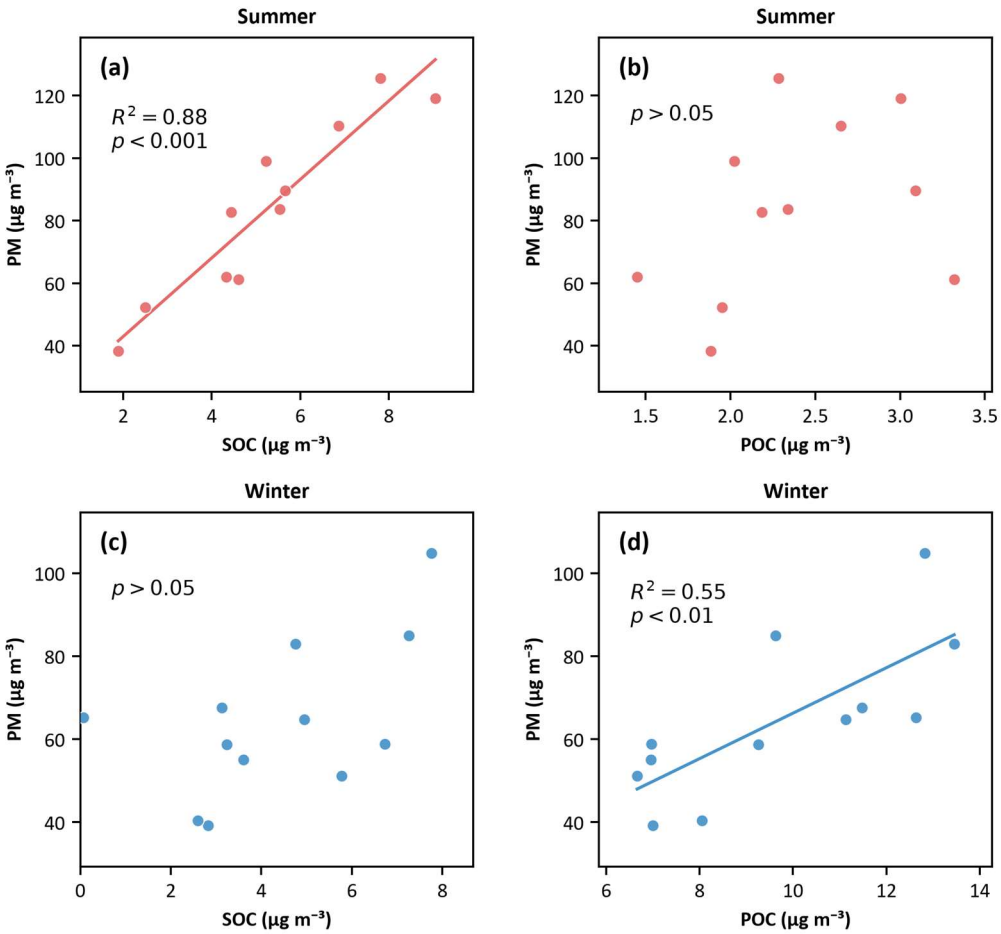


Figure S2. Correlations of PM concentrations with secondary organic carbon (SOC) and primary organic carbon (POC) during summer and winter.

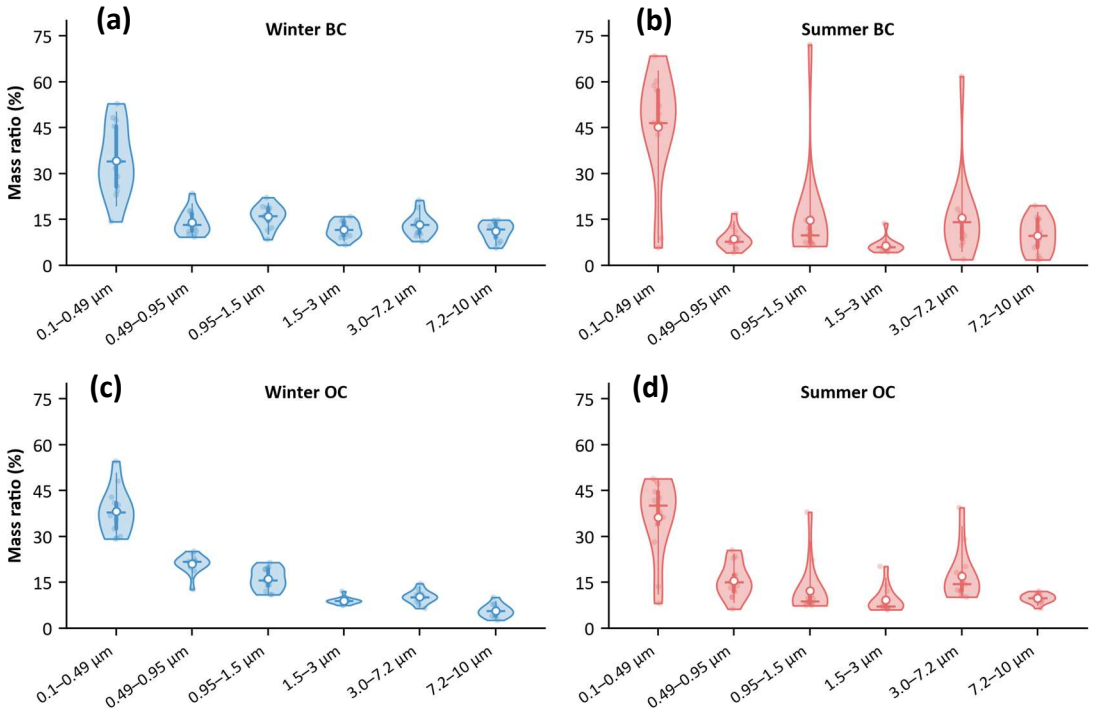


Figure S3. Particle-size distributions of BC and OC mass fractions during winter and summer. Violin plots show the percentage of total BC mass distributed in each particle-size fraction in winter (a) and summer (b), and the corresponding percentage of total OC mass in winter (c) and summer (d). White circles and error bars indicate the mean values and standard deviations, respectively.

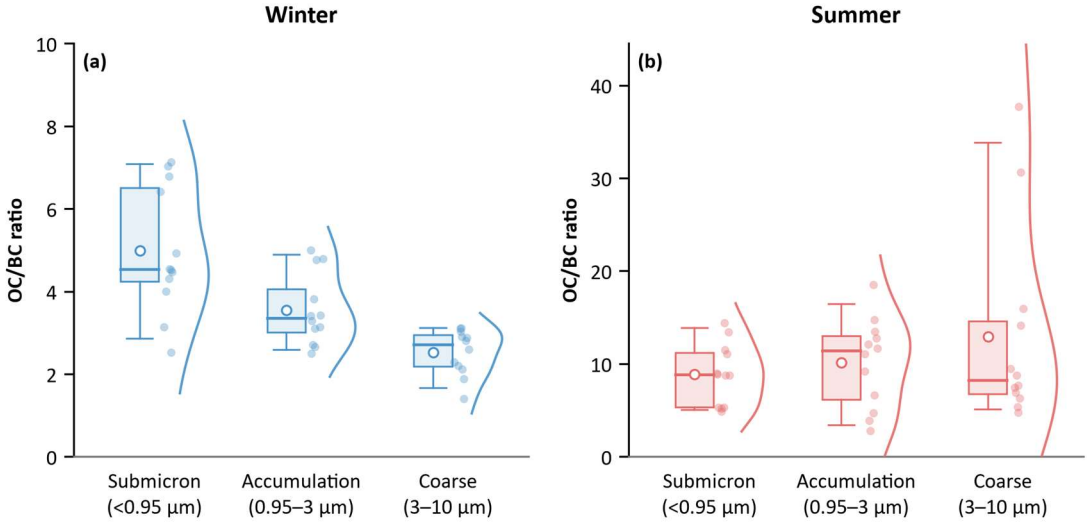


Figure S4. OC/BC ratios in the submicron (<0.95 µm), accumulation (0.95–3 µm), and coarse (3–10 µm) fractions during (a) winter and (b) summer. Boxes represent the interquartile range, horizontal lines indicate the median, open circles denote the mean, and individual points represent separate samples.

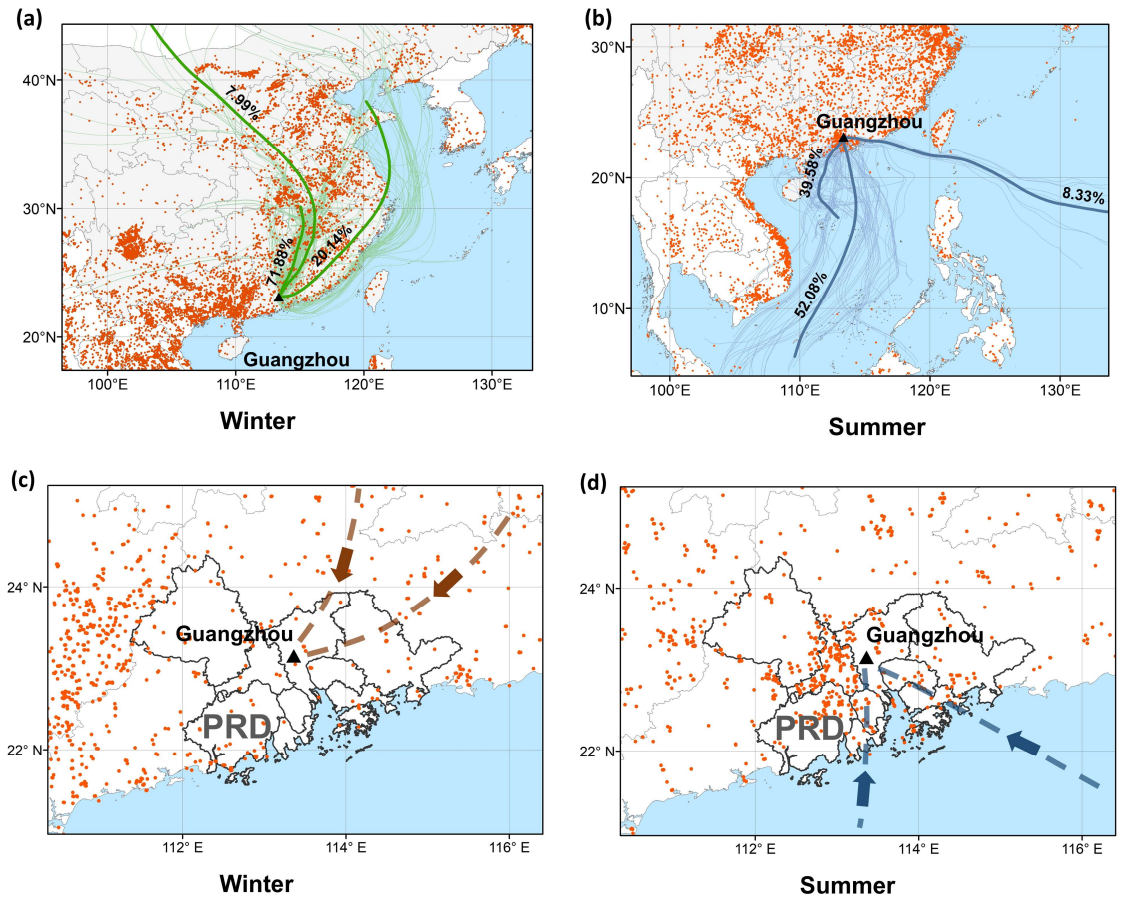


Figure S5. Spatial distributions of active fire hotspots and backward air-mass trajectories reaching Guangzhou during (a) winter and (b) summer. Panels (c) and (d) show the fire hotspot distributions in the Pearl River Delta (PRD) and surrounding areas during winter and summer, respectively. Orange dots represent satellite-detected fire hotspots. In panels (a) and (b), thin lines show individual backward trajectories, while thick colored lines indicate the major trajectory clusters. Percentages indicate the proportion of trajectories assigned to each cluster. Dashed arrows in panels (c) and (d) indicate the prevailing transport directions. Triangles mark the sampling site in Guangzhou.

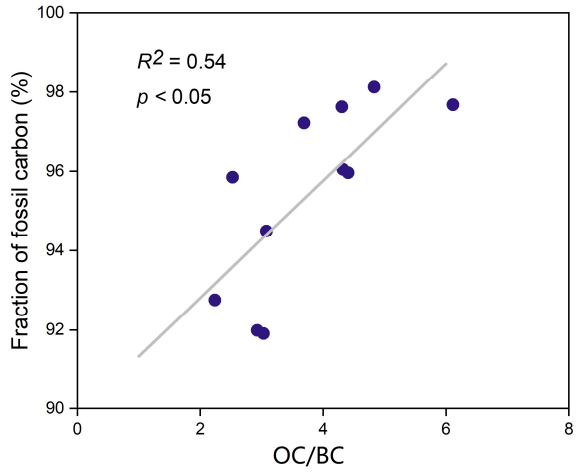


Figure S6. Relationship between the OC/BC ratio and the fossil contribution to BC in the 0.95–1.5 μm particle-size fraction during winter.

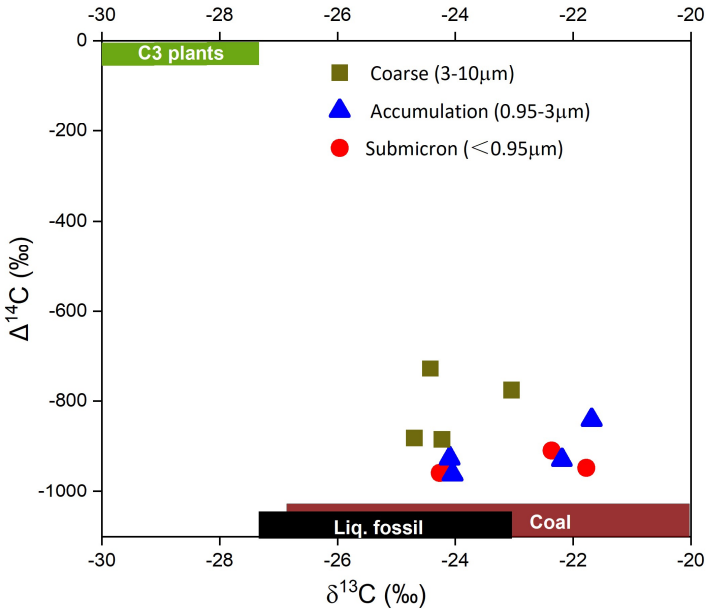


Figure S7. Dual-carbon isotope ($\delta^{13}C$–$\Delta^{14}C$) signatures of BC in the submicron (<0.95 μm), accumulation (0.95–3 μm), and coarse (3–10 μm) fractions.

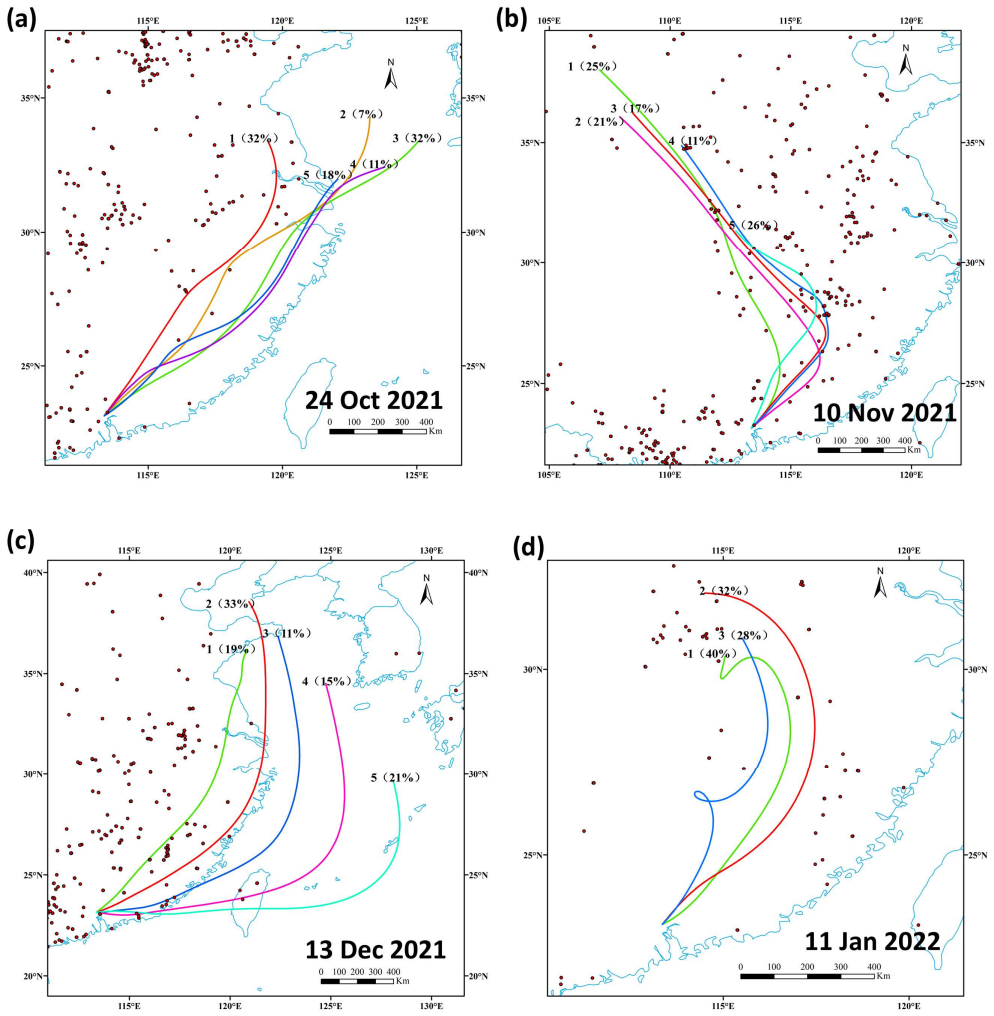


Figure S8. 72h backward air-mass trajectories arriving at Guangzhou at an altitude of 100 m for four representative winter samples collected on (a) 24 October 2021, (b) 10 November 2021, (c) 13 December 2021, and (d) 11 January 2022.